Extracting phonon thermal conductance across atomic junctions: Nonequilibrium Green's function approach compared to semiclassical methods

Patrick E. Hopkins, Pamela M. Norris, Mikiyas S. Tsegaye, and Avik W. Ghosh

Citation: J. Appl. Phys. **106**, 063503 (2009); doi: 10.1063/1.3212974
View online: http://dx.doi.org/10.1063/1.3212974
View Table of Contents: http://jap.aip.org/resource/1/JAPIAU/v106/i6
Published by the American Institute of Physics.

Extracting phonon thermal conductance across atomic junctions: Nonequilibrium Green's function approach compared to semiclassical methods

Patrick E. Hopkins,[1,a] Pamela M. Norris,[2] Mikiyas S. Tsegaye,[3] and Avik W. Ghosh[3]
[1]*Engineering Sciences Center, Sandia National Laboratories, P.O. Box 5800, Albuquerque, New Mexico 87185-0346, USA*
[2]*Department of Mechanical and Aerospace Engineering, University of Virginia, Charlottesville, Virginia 22904, USA*
[3]*Department of Electrical and Computer Engineering, University of Virginia, Charlottesville, Virginia 22904, USA*

(Received 23 March 2009; accepted 1 August 2009; published online 16 September 2009)

The thermal conductance of nanoscale phonon modes is typically calculated using the Boltzmann transport equation. A particular implementation of this method is the acoustic mismatch model (AMM) that compares impedance ratios at a mathematically abrupt transition between two equilibrium regions. The shortcomings of this model can be rectified by starting from a microscopic physics based equation describing the propagation of phonon waves across an extended junction, with carefully computed thermal boundary conditions on either side. The resulting nonequilibrium Green's function (NEGF) formalism provides an accurate yet physically transparent machinery to calculate energy transfer, especially in nanosystems where the concept of thermal equilibrium breaks down readily. The purpose of this paper is to establish the NEGF formalism of thermal conductivity with a few simple examples and illustrate its particular strengths compared to the AMM. © *2009 American Institute of Physics*. [doi:10.1063/1.3212974]

I. INTRODUCTION

The transport of energy across interfaces is a critical area of study in the thermal management of nanosystems.[1] As characteristic lengths of nanomaterials approach the energy carriers' mean free paths, the thermal processes are no longer driven by scattering inside the bulk materials, but are driven instead by scattering at heterojunction interfaces. Thermal transport across an interface is characterized by the thermal conductance per unit area, or the thermal boundary conductance, h_{BD}, that relates the interfacial heat flux, q, to the temperature drop ΔT in linear response via $q=h_{BD}\Delta T$

Accurate predictions of h_{BD} are difficult since transport around interfacial regions is a highly nonequilibrium process and additional scattering mechanisms can greatly complicate analysis. Assuming phonon transport as the dominant mechanism of interfacial thermal transport, one of the most simplified and widely used models for h_{BD} is the acoustic mismatch model (AMM).[2] The AMM is essentially a low temperature model designed for specular elastic scattering of phonons at a perfectly abrupt interface between two materials. Although corrections to these models have been proposed to account for mixing around the interface[3,4] and inelastic scattering,[5–9] many of these suggestions have been *ad hoc* and not derived from a fundamental quantum transport theory for heat flow, disregarding the fundamentally nonequilibrium nature of thermal transport. The formulations of this model are based on a semiclassical formulation of the phonon flux in two materials approaching an interface from either side, assuming the phonon scattering processes at the interface occur abruptly between two separate equilibrium states. The AMM model thus disregards the fact that the energy transition needs to occur over an extended nonequilibruim region whose properties should actually be intermediate between the two thermal "reservoirs" on either side. In addition, the formulation of the AMM, or any semiclassical Boltzmann transport equation (BTE)-based model, does not take into account the wave nature of phonon transport that is driven by the underlying lattice dispersion and the boundary conditions on either side. There is no straightforward way to extend this model to nanostructures with multiple interfaces, where multiple reflection and phase coherence of confined phonon waves is anticipated to be critical to thermal processes.

In this work, the nonequilibrium Green's function (NEGF) approach[10,11] is used to study phonon thermal transport and energy transmission across adjacent materials in one-dimensional (1D) atomic chains. The NEGF formalism arises out of a microscopic theory of nonequilibrium processes[12] and couples the equations of motion of the atoms with the nonequilibrium thermodynamics at their boundaries.[13] Being ultimately a matrix equation in a given basis set, the technique can be expanded to far-from-equilibrium quantum transport across extended physical junctions, leading to prominent quantum signatures in the transmission.

The NEGF formalism has been extensively used to study quantum electron transport in nanoscopic systems,[10,14–17] especially for quasiballistic devices where characteristic wavelengths of the electron system become comparable to, or larger than, the sample dimensions. The method can be readily adapted to include incoherent scattering and weak

[a]Author to whom correspondence should be addressed. Electronic mail: pehopki@sandia.gov.

electron and phonon correlation effects. Following the recent experimental verification of the low temperature quantum of thermal conductance[18] ($\lambda_0=\pi^2k_B^2T/3h$, where k_B is Boltzmann's constant, T is the carrier temperature, and h is Planck's constant), significant effort has been delegated on adapting this formalism to phonon transport in nanosystems and low dimensional structures.[19–26] Our aim in this paper is to derive these equations for simple systems and illustrate the role of quantum effects in phonon thermal conductance.

An excellent walkthrough of the general NEGF formulation is given by Zhang *et al.* and example calculations are given for 1D atomic chains.[24] Besides illustrating the superiority of NEGF with more well established semiclassical models, the role of the present work is to develop the simplest application of thermal NEGF—a single atom "device," illustrated with a "toy model" paralleling its electronic counterparts.[27] The real strength of NEGF is its ability to handle more complicated incoherent scattering such as anharmonic phonon processes. Under strong drive currents, stronger nonperturbative many-body correlation effects can arise, which would even require going beyond NEGF. Such complexities (incoherence and correlation) actually carry interesting physics and could be critical for nanosystems. In the interest of simplicity, however, we leave these issues for future publications, restricting ourselves to elastic flow. We also grossly simplify the phonon bandstructure by working with a single[28] sinusoidal longitudinal phonon mode.

II. SEMICLASSICAL MODELS

The starting point for many semiclassical thermal boundary models is a population of bulk phonons approaching the interface between two materials.[29] This concept is based on the parallel between phonon transport and radiative photon transport. Treating the phonons as wavepackets of energy, their spectral intensity is defined as

$$I_j = v_j f_j(\omega,T)\hbar\omega D_j(\omega), \tag{1}$$

where $\hbar$ is Planck's constant divided by 2π, ω is the phonon vibrational angular frequency, v_j is the group velocity of phonons with polarization j (longitudinal or transverse) within some to-be-defined solid angle approaching the interface, and $D_j(\omega)$ is the spectral phonon density of states of polarization j per unit volume. The phonon distribution function is represented by $f(\omega,T)$, which, in these semiclassical analyses, is taken as the equilibrium Bose–Einstein distribution function. In the case of a three-dimensional (3D) medium, the expression for phonon intensity in Eq. (1) is often divided by a factor of 4π assuming an isotropic 3D medium;[30] since this work focuses on conductance in 1D wires, this factor is not needed. In addition, in this 1D consideration, atoms are restricted to move along the direction of thermal transport, so only one longitudinal mode is considered. With Eq. (1) for phonon intensity, the incident heat flux of phonons impinging on the interface of two atoms in a 1D chain can be defined as[30]

$$q = \int_0^{\omega_c} I d\omega, \tag{2}$$

where ω_c is the phonon cutoff frequency of the longitudinal phonon mode.

In order to determine the heat flow across the interface, Eq. (2) must be related to the definition for thermal conductance, given by

$$\Delta q = h_{BD}\Delta T, \tag{3}$$

where Δq represents the net heat flux across the interface, $\Delta q=q_{ab}-q_{ba}$, where q_{ab} and q_{ba} are the gross heat fluxes transmitted across the interface from side a to side b and from side b to side a, respectively. The heat fluxes in turn are defined as

$$q_{ab} = \int_0^{\omega_{c,a}} t_{ab} v_a f_a \hbar\omega D_a d\omega, \tag{4}$$

where t_{ab} is the phonon transmissivity from side a to side b (a similar formulation for q_{ba} is given by this equation). We thus have

$$\Delta q = \int_0^{\omega_{c,a}} t_{ab} v_a f_a \hbar\omega D_a d\omega - \int_0^{\omega_{c,b}} t_{ba} v_b f_b \hbar\omega D_b d\omega. \tag{5}$$

The principle of detailed balance states that at equilibrium $\Delta q=0$, so that Eq. (5) can be rearranged to[31]

$$\Delta q = \int_0^{\omega_{c,a}} t_{ab} v_a (f_a - f_b)\hbar\omega D_b d\omega. \tag{6}$$

Equation (6) takes the form of the familiar Landauer formalism that treats thermal transport as transmission of phonons between two infinitely large reservoirs at two different temperatures.[32] Equation (6) can then be related to the thermal boundary conductance through Eq. (3). In the limit of $\Delta T=0$, when the flux is evaluated at the interface and not over an extended interface specific region between two reservoirs, Eq. (6) reduces to an expression for thermal boundary conductance, given by

$$h_{BD} = \int_0^{\omega_{c,a}} t_{ab} v_a \frac{\partial f}{\partial T} \hbar\omega D_a d\omega. \tag{7}$$

The assumption of equilibrium, which allows for the application of the principle of detailed balance, relates the two phonon heat fluxes on either side of the interface by assuming that there is no net heat flow across the interface. This assumption of local equilibrium around the interface has serious implications in phonon transmission probability calculations. When applying detailed balance to the phononic heat fluxes, the two incoming fluxes are assumed at the same temperature. In this equilibrium condition, the phonon systems around the interface are statistically described by the same Bose–Einstein distribution function and not a nonequilibrium distribution. This causes a discontinuity between the Fourier Law and interfacial heat flux predicted with Eq. (7).[33]

Assuming complete specular scattering, we can use AMM theory to extract the transmission, which is a function of the acoustic impedance, Z, on either side of the interface[2]

$$t_{ab}^{\mathrm{AMM}} = \frac{4Z_aZ_b}{(Z_a+Z_b)^2} = \frac{4\rho_a v_a \rho_b v_b}{(\rho_a v_a + \rho_b v_b)^2}, \tag{8}$$

where ρ is the volumetric mass density of the material on the specified side. This 3D form is inappropriate for a 1D chain and should be slightly modified to take into account a length mass density instead of the volumetric mass density, so that Eq. (8) becomes

$$t_{ab}^{\mathrm{AMM}} = \frac{4\frac{M_a}{d_a}v_a\frac{M_b}{d_b}v_b}{\left(\frac{M_a}{d_a}v_a + \frac{M_b}{d_b}v_b\right)^2}, \tag{9}$$

where M is the mass of the atom and d is the interatomic spacing between the atomic masses. In the case of acoustic scattering when the atoms on either side of the interface are identical, both Eqs. (8) and (9) reduce to unity. To calculate the thermal boundary conductance, h_{BD}, and the subsequent phonon transmission probability, t_{ab}^{AMM}, the phonon dispersion must be defined. A sine-type dispersion is assumed for the 1D phonon chain,[28,34]

$$\omega = \omega_c \sin\left|\frac{kd}{2}\right|, \tag{10}$$

where k is the wavevector. The phonon velocity along the atomic chain anywhere in the Brillouin zone is then given by its slope $v=\partial\omega/\partial k$, while its density of states per unit length is given by $D=1/2\pi v$.[34] Finally, the expression for thermal boundary conductance at a single atom interface, Eq. (7) becomes

$$\lambda_{BD} = \frac{\hbar}{2\pi}\int_0^{\omega_{c,a}} t_{ab}\frac{\partial f}{\partial T}\omega d\omega, \tag{11}$$

where the velocities calculated from Eq. (10) are incorporated into Eq. (9) for the transmission and only frequencies up to the lowest cutoff frequency of the two materials are retained for elastic scattering. The transmission at the heterointerface thus depends on material properties such as the masses and dispersion parameters (resonant frequencies, interatomic separations, etc.). For the limit of homojunctions, it is straightforward to show that we recover the quantum of thermal conductance. Inserting the Bose–Einstein distribution function into Eq. (11) yields

$$\lambda = \frac{\hbar}{2\pi}\int_0^{\omega_{c,a}}\frac{\partial f}{\partial T}\omega d\omega = \frac{\hbar^2}{2\pi k_B T^2}\int_0^{\omega_{c,a}}\omega^2\frac{\exp\left[\frac{\hbar\omega}{k_BT}\right]}{\left(\exp\left[\frac{\hbar\omega}{k_BT}\right]-1\right)^2}d\omega. \tag{12}$$

At low temperatures ($T \ll \theta_D$, where θ_D is the Debye temperature), the upper limit of the integral in Eq. (12) can be extended to infinity and solved exactly, giving

$$\int_0^{\infty}\omega^2\frac{\exp\left[\frac{\hbar\omega}{k_BT}\right]}{\left(\exp\left[\frac{\hbar\omega}{k_BT}\right]-1\right)^2}d\omega = \frac{\pi^2k_B^3T^3}{3\hbar^3}, \tag{13}$$

so that Eq. (12) yields the material independent quantum conductance per phonon mode[18]

$$\lambda_0 = \frac{\pi^2k_B^2T}{3h}. \tag{14}$$

III. 1D NEGF FORMULATIONS

As previously mentioned, the AMM makes the unphysical assumption of thermal equilibrium achieved immediately on either side of a single abrupt junction.[20] In other words, there is no clear recipe on how to combine individual impedances for an extended channel region driven into nonequilibrium by two separate thermal reservoirs, as is commonly invoked for electron flow. Electron flow is usually formulated as a two-junction problem, making a clear conceptual separation between "contacts" that are held at separate thermal equilibria by a battery, aided by inelastic thermalizing scattering events in them, and a "channel" or "device" region where the actual transport dynamics occurs. The viewpoint leads naturally to the NEGF technique, which is now part of the device theorists' toolkits.

The clear separation of the dynamics (channel) from the thermodynamics (contacts) allows us to set up a wave equation for quantum transport with precise boundary conditions imposed by the reservoirs, so that local physical quantities, such as the nonequilibrium phonon density and the thermal current, can be explicitly calculated. The NEGF approach for phonon transport proceeds analogously in two steps: first the phonon propagation equations for the contacts are partitioned out to create an equivalent open-boundary version of Newton's law for lattice vibrations in the channel.[34] The contact states enter their boundary condition through carefully computed self-energy matrices. Next, a thermal equilibrium condition is imposed on the contact state bilinear variables in order to compute the NEGF thermal current. Assuming an infinite 1D chain of atoms each with masses M_a and spring constants K_a, as illustrated in Fig. 1(a), we get the dispersion relation presented in Eq. (10), where the cutoff frequency, ω_c, is given by

$$\omega_c = 2\sqrt{\frac{K_a}{M_a}}. \tag{15}$$

These results assume an atomic displacement of the nth atom in the chain, $u_{n,a}$, in the form of a plane wave solution given by

$$u_{n,a} = u_0\exp[i(knd_a)]. \tag{16}$$

These same assumptions will be made when going through the NEGF formulations. In addition, this analysis will only consider an atomic chain with a single point basis (i.e., no optical phonons), which is valid here since optical phonons do not participate significantly in thermal transport due to their low group velocity.

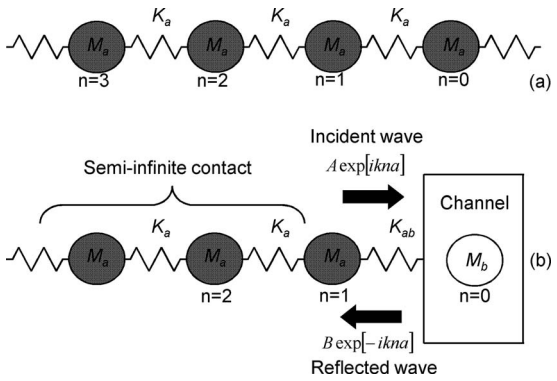

FIG. 1. (a) Infinite 1D chain of atoms with mass M_a and spring constant K_a. Assuming plane wave solutions give rise to the dispersion relation given by Eq. (10). (b) Assuming an atom in the "channel" that is different from the atoms in the contact yields a modified spring constant at the contact/channel interface and gives rise to incident and reflected waves.

A. Left contact–single atom channel

In this section, Newton's law with an open boundary condition for a single junction is worked out. Consider a linear semi-infinite 1D chain of atoms of material a (contact) connected at the right end to a single channel atom of material b; the atoms in the contact have mass M_a and spring constant K_a between the contact atoms, the channel is a single atom of mass M_b, the spring constant in between the contact and channel is given by K_{ab}, and the distance between the contact and channel atom is assumed as the interatomic spacing between the contact atoms, d_a. Denoting the channel atom as coordinate 0 and the atoms of material a with coordinate $(n=1,2,\cdots)$ with $n=1$ being the surface atom next to b (Fig. 1), the equations of motion governing the various atoms are given from Hooke's law as

$$F_0 = -M_b\omega^2 u_0 = K_{ab}(u_1 - u_0) \tag{17}$$

and

$$F_a = -M_a\omega^2 u_n = K_a(2u_n - u_{n-1} - u_{n+1}). \tag{18}$$

We expect to see plane waves propagating in both directions inside the contact due to interfacial reflection, yielding a planar contact wave of the form $u_n = B\exp[iknd_a] + C\exp[-iknd_a]$. Assuming wave solutions of this form we get the standard dispersion [Eq. (10)] for the 1D contact. In addition, we get the following displacement equations for the contact atom and the channel surface atom:

$$u_0 = B + C \tag{19}$$

and

$$u_1 = B\exp[ikd_a] + C\exp[-ikd_a]. \tag{20}$$

The goal of the NEGF approach is to replace the semi-infinite contact with a source term incident on the channel and a self-energy that affects the energy of the channel, in this case, atom b. Therefore, the displacement of material a atom in position 1 must be expressed in terms of the incident wave only and not the reflected wave, so that the semi-infinite contact can be treated as an incident source term, S, that takes into account reflection with a self-energy, Σ, both of which affect the channel atom. Combining Eqs. (19) and (20) yields,

$$u_1 = -2iB\sin[kd_a] + \exp[ikd_a]u_0 \tag{21}$$

and inserting Eq. (21) into Eq. (17) yields

$$-M_b\omega^2 u_0 = K_{ab}(-2iB\sin[kd_a] + \exp[ikd_a]u_0 - u_0), \tag{22}$$

which is rearranged to give the open-boundary Newton's Law

$$(M_b\omega^2 - K_{ab} - \Sigma_{ab})u_0 = S_{ab}, \tag{23}$$

where

$$\Sigma_{ab} = -K_{ab}\exp[ikd_a] \tag{24}$$

is the self energy of the contact acting as an energy-dependent boundary condition for the channel and

$$S_{ab} = 2iBK_{ab}\sin[kd_a] \tag{25}$$

is the source term representing the excitation of the channel atoms driven by atomic vibrations in the contact. Note that the self-energy, Σ_{ab}, and the source, S_{ab}, are dependent on the spring force, K_{ab}, and not the masses in the contact, M_a. The solution to Eq. (23) is given by

$$u_0 = S_{ab}G, \tag{26}$$

where G is the retarded Green's function for the *channel*, which in this example gives the effects of the contact on the channel atom, given by

$$G = [M_b\omega^2 - K_{ab} - \Sigma_{ab}]^{-1}. \tag{27}$$

Rearranging Eq. (10), the wavevector k can be expressed in terms of ω as

$$k = \frac{2}{d_a}\sin^{-1}\left(\frac{\omega}{\omega_{c,ab}}\right), \tag{28}$$

where $\omega_{c,ab}$ is the modified cutoff frequency at the contact/channel interface due to the different masses and spring constants of the contact atoms and channel atom, and substituting Eq. (28) into Eq. (24) and then Eq. (27) gives the Green's function in terms of angular phonon frequency.

The self-energy of the contacts, Σ_{ab}, affects the dispersion around the interface and creates a frequency broadening described by

$$\Gamma_{ab} = i(\Sigma_{ab} - \Sigma_{ab}^{+}), \tag{29}$$

where the superscript "+" refers to the conjugate transpose of Σ. In this simple 1D example,

$$\Gamma_{ab} = 4K_{ab}\left(\frac{\omega}{\omega_{c,ab}}\right)\sqrt{1 - \left(\frac{\omega}{\omega_{c,ab}}\right)^2} \tag{30}$$

In general, the self-energy, Σ_{ab}, written explicitly in Eq. (24), can also be related to the surface Green's functions of the left contact g_{ab},[27] via

$$\Sigma_{ab} = \tau_{ab}g_{ab}\tau_{ab}^{+} \tag{31}$$

where τ_{ab} is the thermal coupling term between the left contact and the channel (atoms a and b) and g is the surface

element of the *contact* Green's function., Finally, the channel density of states is obtained by tracing over the spectral function of the channel, A,[27] which can be defined as

$$A = i[G - G^+] = G\Gamma_{ab}G^+ = \frac{4K_{ab}\left(\frac{\omega}{\omega_{c,ab}}\right)\sqrt{1-\left(\frac{\omega}{\omega_{c,ab}}\right)^2}}{(M_b\omega^2)^2 + 4K_{ab}\left(\frac{\omega}{\omega_{c,ab}}\right)^2(K_{ab} - M_b\omega^2)}, \quad (32)$$

where Γ_{ab}, in addition to Eq. (30), is given by

$$\Gamma_{ab} = \tau_{ab}A_{ab}\tau_{ab}^+. \quad (33)$$

The spectral function being related to Γ suggests that A is related to the local density of states at the contact/channel interface.

The process described above can be readily extended to two contacts and a channel. Assuming that the contacts are of the same material, then the Green's function for this system becomes

$$G = [M_b\omega^2 - 2K_{ab} - 2\Sigma_{ab}]^{-1}. \quad (34)$$

The expression $2K_{ab}$ is the sum of the two spring constants on either side of the atom that restores the atom to its equilibrium position after the perturbation from the Σ_{ab} wave on either side of the atom.

B. Local density of states and transmission

The development of the nonequilibrium Green's function, G, self-energy of the contact, Σ, source term, S, frequency broadening term, Γ, and spectral function of the channel, A, in this section exactly parallels the development of these analogous terms for electronic transport derived in the toy examples in Secs. 8.1 and 9.2 of Datta.[27] The difference between this approach to phonon transport and the approach outlined by Zhang *et al.*[24] is how the interactions between atoms are conceptually viewed. Instead of using spring constants, K, to describe all the interactions, Zhang *et al.* develops all key equations using a harmonic term (the work of Zhang *et al.* develops the theory in 3D, so they actually use a harmonic matrix), which is just the spring constant between two masses (e.g., K_{ab}) divided by the square root of the product of the two masses (e.g., $\sqrt{M_aM_b}$), so that the harmonic term, H, in this example would be given by

$$H = \frac{K_{ab}}{\sqrt{M_aM_b}}. \quad (35)$$

Dividing Eq. (34) by $\sqrt{M_aM_b}$ gives the same Green's function developed by Zhang *et al.*

Returning now to the density of states, the spectral function, A, is related to the local spectral density of states, $\mathcal{D}$, via

$$A = 2\pi\mathcal{D}, \quad (36)$$

where $\mathcal{D}$ is related to the phonon density of states, D, by

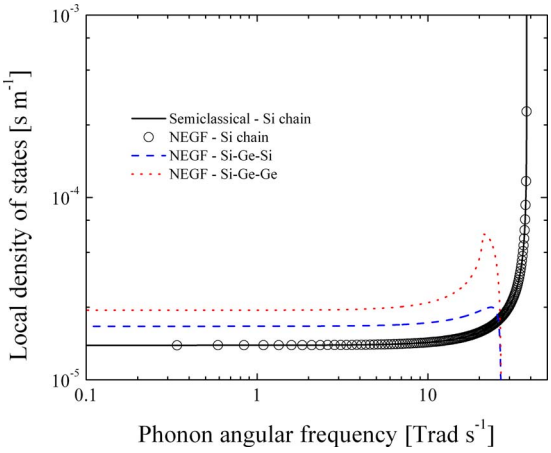

FIG. 2. (Color online) Density of states of a 1D chain of Si atoms calculated with $D=1/2\pi v$ (semiclassical) and compared to calculations using the NEGF formalism [Eq. (37)]. The two formalisms for calculating the density of states are directly compared by assuming Si contacts and a single atoms Si channel in the NEGF calculations. The NEGF formalism gives the ability to calculate the local density of states of a single atom in a structure, such as a single Ge atom channel connected to Si contacts, as shown by the blue dashed line, or a single Ge atom connected to a Si contact and a Ge contact, as shown by the red dotted line.

$$D = \frac{\mathcal{D}\omega\sqrt{M_aM_b}}{d_a}, \quad (37)$$

so that the density of states describing the contact-channel vibrations is given by

$$D = \frac{\omega A\sqrt{M_aM_b}}{2\pi d_a} = \frac{\omega i[G - G^+]\sqrt{M_aM_b}}{2\pi d_a} = \frac{4K_{ab}\left(\frac{\omega^2}{\omega_{c,ab}}\right)\sqrt{M_aM_b}\sqrt{1-\left(\frac{\omega}{\omega_{c,ab}}\right)^2}}{\pi d_a\left((M_b\omega^2)^2 + 8K_{ab}\left(\frac{\omega}{\omega_{c,ab}}\right)^2(2K_{ab} - M_b\omega^2)\right)}. \quad (38)$$

Note that Eq. (38) differs from the density of states presented by Zhang *et al.* by a factor of 1/2. This is due to the assumption of "positive" phonon transport and hence only half of the Brillouin zone is considered. Note that assuming the same atom in the channel as in the contact gives the same calculations as the semiclassical density of states described in Sec. II, $D=1/2\pi v$. Similarly, the density of states for the channel atom with two different contact materials is given by using Eq. (37) and averaging the square root of the product of the atomic masses of the channel atom and the adjacent atoms.

Figure 2 presents the calculation of the density of states given by Eq. (37) assuming: (1) the contacts and the single atom channel are the same material (both Si atoms), (2) the contacts are comprised of Si atoms and the single atom channel is a Ge atom, and (3) one contact is Si and the other Ge with the single atom Ge channel. The semiclassical density of states calculations are also shown for a Si 1D chain. For simplicity in all calculations in this work, the interatomic spacing is assumed as the interatomic spacing of Si. The interatomic forces used to estimate the spring constant, K,

TABLE I. Elastic and atomic properties of Au, Ge, and Si. The interatomic spacing, d, and the elastic constant, c_{11}, and mass of a single atom, M, are taken from the literature (Ref. 36). The mass used in the calculations in this study is M times the atomic basis, r. The spring constant, K, listed here is calculated via Eq. (40) assuming a homogeneous chain. The spring constant between two different atoms is estimated by averaging the elastic constants of the two materials (c_{11}) and using the averaged c_{11} in Eq. (40).

	Units	Ge	Si
d	nm	0.566	0.543
c_{11}	N m^{-2}	12.92×10^{10}	16.57×10^{10}
K	N m	13.7	16.9
M	kg	1.2×10^{-25}	4.7×10^{-26}
r		2	2

are calculated from the second derivative of the interatomic potential, where Harrison's interatomic potential is assumed, given by[35]

$$\Delta U = \frac{1}{2}C_0\frac{u^2}{d^2} + \frac{1}{2}C_1(\Delta\theta)^2, \tag{39}$$

where C_0 and C_1 are interatomic force constants. In the 1D chains, the change in the equilibrium tetrahedral angle, $\Delta\theta$, is irrelevant and zero. The spring constants, K, result from the second derivative with respect to u and therefore are described by

$$K = \frac{C_0}{d^2}, \tag{40}$$

where, for a 3D system, C_0 is a function of the elastic constants given by[35]

$$C_0 = \frac{3d^3}{16}(c_{11} + 2c_{12}), \tag{41}$$

and c_{11} and c_{12} are the elastic constants of the corresponding bulk material. For a 1D chain, Eq. (41) should not include any transverse interactions, so Eq. (41) becomes

$$C_0 = \frac{3d^3}{16}c_{11}. \tag{42}$$

By substituting Eq. (42) into Eq. (40), the spring constant expression becomes

$$K = \frac{3dc_{11}}{16}. \tag{43}$$

Although K in Eq. (43) is based on a 3D crystal potential, this approximation will be used for K in this simple example to extract the fundamental physical trends related to phonon conductance. When two different atoms are adjacent to each other, such as the Si contact and Ge single atom channel, the spring constant, K_{ab}, is estimated by averaging the elastic constants of the two materials and the cutoff frequency is estimated by K_{ab} and averaging the atomic masses. (In a proper atomistic model, one will need to compute these interfacial spring constants from the exact dynamical matrices.) Table I lists the elastic and atomic parameters of Si and Ge pertinent in this study.[36]

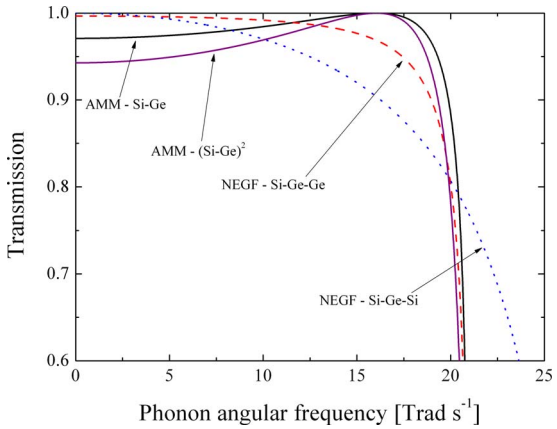

FIG. 3. (Color online) Transmission across the single atom channel, as predicted by NEGF calculations [Eq. (44)], compared to transmission across an atomic interface using the 1D AMM formulation [Eq. (9)]. The transmission across a single atom Ge channel connected to a 1D Si and Ge contact (NEGF-Si–Ge–Ge) is compared to the AMM transmission assuming a single Si–Ge interface. The transmission across a single atom Ge channel connected to 1D Si contacts on either side (NEGF-Si–Ge–Si) is compared to the AMM formulation by squaring the AMM transmission for a Si–Ge interface [AMM-(Si–Ge)^2].

With the local density of states of the channel atom defined, the task now is to define the transmission probability using the nonequilibrium Green's function of the system. The transmission probability can be calculated by[27]

$$t_{abc}^{\mathrm{NEGF}} = \mathrm{Trace}[\Gamma_{ab}G\Gamma_{bc}G^{+}], \tag{44}$$

which, for this single atom channel example, when the contacts are both the same material, is simply

$$t_{aba}^{\mathrm{NEGF}} = \Gamma_{ab}G\Gamma_{ba}G^{+}. \tag{45}$$

Figure 3 shows the transmission probabilities as a function of frequency using the NEGF transmission and the AMM transmission in Eq. (9). The transmission at a single Si–Ge atomic junction is compared with AMM predictions (AMM-Si–Ge) and NEGF predictions (NEGF-Si–Ge–Ge). These calculations, for the same interface and geometry, are different using the two methods of calculation. Calculations of the AMM only consider the materials on either side of the interfacial bond and not the interfacial bond itself, such as bond between the Si and Ge atoms. This bond at the atomic interface however drives interfacial transport and scattering. The NEGF formalism, however, calculates transport across the channel, in this case, the Ge atom, and therefore takes into account masses and forces (bond strengths) on either side of the channel atom. In this NEGF calculation case of a Si and a Ge contact on either side of a single atom Ge channel, the force that causes interfacial transmission to deviate from unity is that between the Si contact and Ge channel. Note, for the NEGF transmission calculations, the spring constant between the Si–Ge atoms is estimated by averaging the elastic constants, as described above. The shape and trends of the NEGF transmission for the Si–Ge interface are intuitively more physical than that of the AMM transmission. At low frequencies, the Ge channel atom can vibrate at the same frequency as the contacts and so transmission at these frequencies should be unity, as predicted by NEGF but not

the AMM. As the frequency approaches the maximum vibrational frequency of the Si–Ge atomic bond, the transmission decreases to zero. The AMM predicts an increase in transmission to unity before decreasing to zero. This is a nonphysical consequence of the AMM formulation. As the phonon frequency approaches that of the Ge cutoff frequency, the term describing the Ge acoustic impedance in the AMM transmission equation [Eq. (9)] becomes negligible compared to the term describing the Si impedance, and so the transmission slowly increases to unity, after which, the Ge term rapidly approaches zero causing the transmission probability to go to zero. This nonphysical aspect is not present in the NEGF calculations of transmission, which shows a slowly decreasing transmission as frequency increases to that of the Ge cutoff frequency, which is expected assuming only elastic phonon transmission. Also shown in Fig. 3 are calculations for transmission assuming Si contacts and a Ge single atom channel. The NEGF calculation on this geometry naturally takes into account forward and backward propagating waves across the Ge atom as a result of scattering at the two Ge–Si junctions. The straightforward way to take this into account in the traditional AMM formulation would be to model this scenario as transmission across two isolated interfaces, effectively Eq. (9) squared for a Si–Ge junction.

IV. NEGF CALCULATIONS OF THERMAL CONDUCTANCE

The transmission allows us to compute the thermal conductance by Taylor expanding the Landauer equation

$$q = \frac{\hbar}{2\pi}\int_0^{\omega_c} t_{abc}^{\mathrm{NEGF}}(f_a - f_c)\omega d\omega, \tag{46}$$

where f_a and f_c are the semi-infinite contacts of material a and c, respectively, and ω_c is the cutoff frequency of the system assuming only elastic scattering and transmission. Note that although the ingredients in this equation are calculated using open boundary Newton's law, the conductance equation itself is quantum mechanical, as it apportions a fixed phase space for each thermal mode. As the two contacts approach the same temperature, a length independent thermal conductance, l, of the 1D chain is expressed in the NEGF formalism by

$$\lambda_{\mathrm{NEGF}} = \frac{\hbar}{2\pi}\int_0^{\omega_c} t_{abc}^{\mathrm{NEGF}}\frac{\partial f}{\partial T}\omega d\omega. \tag{47}$$

Note the only difference between Eqs. (47) and (11) lies in the calculation of the transmission coefficient, which was discussed in detail in the previous sections.

Figure 4 shows conductance calculations across a single atom junction for the different scenarios presented in Fig. 3. As expected from the transmission calculations, when a Si–Ge scattering event is introduced into a Si chain, it decreases the thermal conductance. In the situation of a single Si–Ge atomic junction, the NEGF and AMM formulations predict noticeably different conductances. In the event of a single atom Ge channel connected to two Si contacts, the conductance predicted by the AMM only slightly decreases. However, there is a noticeable decrease in the NEGF formulation from the Si–Ge–Ge geometry to the Si–Ge–Si geometry. This is due to the transmission calculations discussed in the previous section.

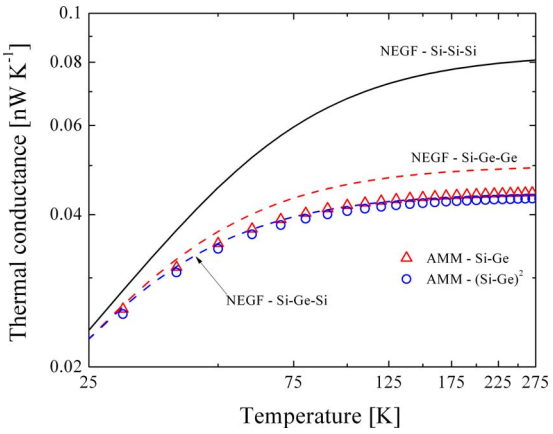

FIG. 4. (Color online) Thermal conductance calculations using Eq. (47) for the NEGF calculations or Eq. (11) for the AMM calculations [note, Eqs. (11) and (47) only differ by the prescribed transmission to use in the calculation, otherwise, these equations are identical] with the various transmission calculations in Fig. 3. In addition, the thermal conductance of a Si channel (transmission of unity) is shown. The NEGF calculations are shown by the dashed lines, the AMM calculations by the symbols, and the Si homogeneous chain calculation by the solid line.

Thus far, this work only focused on a single atom channel. However, the NEGF formalism, as derived for the single atom channel, can easily be extended to a channel containing multiple atoms. Consider a multiple atom 1D channel. In this case, the terms in Green's function and transmission for the device become square matrices of dimension N. Green's function becomes

$$\tilde{G} = [\tilde{M}\omega^2 - \tilde{K} - \tilde{\Sigma}_{ab} - \tilde{\Sigma}_{bc}]^{-1}, \tag{48}$$

where $\tilde{M}$ is the matrix of masses in the channel, $\tilde{K}$ is the matrix of spring constants, and $\tilde{\Sigma}_{ab}$ and $\tilde{\Sigma}_{bc}$ are the self-energy matrices describing the left and right contacts, respectively. The mass matrix for the channel is given by

$$\tilde{M} = \begin{bmatrix} M_{1,1} & 0 & \cdots & 0 \\ 0 & M_{2,2} & 0 & \vdots \\ \vdots & 0 & \ddots & \vdots \\ 0 & \cdots & \cdots & M_{N,N} \end{bmatrix}, \tag{49}$$

where $M_{j,j}$ is the mass of atom at position j in the 1D channel. The matrix of spring constants is given by

$$\tilde{K} = \begin{bmatrix} 2K_{1,1} & -K_{1,2} & \cdots & 0 \\ -K_{2,1} & 2K_{2,2} & -K_{2,3} & \vdots \\ \vdots & -K_{3,2} & \ddots & \vdots \\ 0 & \cdots & \cdots & 2K_{N,N} \end{bmatrix}, \tag{50}$$

where $K_{j,i}$ describes the spring constant of between the atom at position j and the atoms at position $j-1$ and $j+1$ and $2K_{j,j}$ is proportional to the restoring force of the atom at position j from the two atoms on either side ($j-1$ and $j+1$). There is no spring constant in Eq. (50) acting to the left and right of the atoms at position 1 and N in the N atom channel since these are described by the self-energy matrices, which are given by

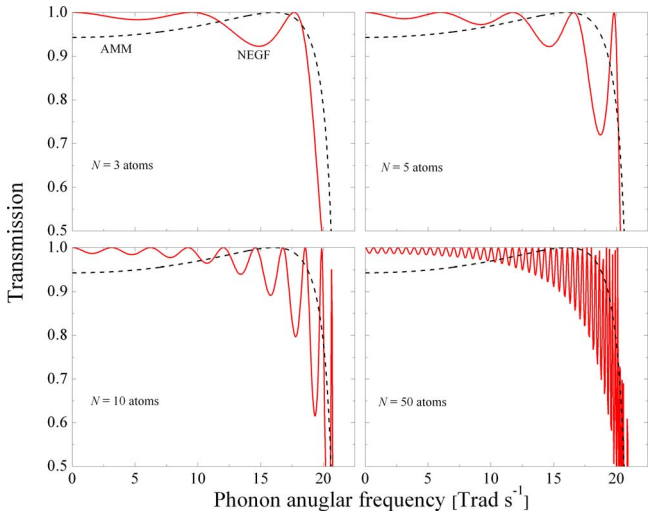

FIG. 5. (Color online) Transmission calculations for a Ge 1D channel connected to Si contacts. For different lengths for the Ge channel are shown: N=3, 5, 10, and 50 atoms. The NEGF calculations are shown by the solid lines and the AMM calculations are the dashed lines. Note the AMM transmission is identical for each case since the AMM calculations only consider transmission of the phonon energy across the two Si–Ge contact/channel junctions. The NEGF calculations, however, take into account phonon reflection and transmission across the junctions and account for wave interference. This is evident from the Fabry–Pérot-like peaks occurring at given frequencies. The number of peaks is related to the number of atoms in the channel.

$$\tilde{\Sigma}_{ab} = \begin{bmatrix} \Sigma_{ab} & 0 & \cdots & 0 \\ 0 & 0 & 0 & \vdots \\ \vdots & 0 & \ddots & \vdots \\ 0 & \cdots & \cdots & 0 \end{bmatrix} \tag{51}$$

and

$$\tilde{\Sigma}_{bc} = \begin{bmatrix} 0 & 0 & \cdots & 0 \\ 0 & 0 & 0 & \vdots \\ \vdots & 0 & \ddots & \vdots \\ 0 & \cdots & \cdots & \Sigma_{bc} \end{bmatrix}, \tag{52}$$

where Σ_{ab} and Σ_{bc} are described by Eq. (24). Now the energy level broadening matrix is given by

$$\tilde{\Gamma}_{ab/bc} = i(\tilde{\Sigma}_{ab/bc} - \tilde{\Sigma}^{+}_{ab/bc}), \tag{53}$$

so the transmission across the channel is given by

$$t^{\mathrm{NEGF}}_{aba} = \mathrm{Trace}[\tilde{\Gamma}_{ab}\tilde{G}\tilde{\Gamma}_{bc}\tilde{G}^{+}]. \tag{54}$$

The transmission calculations using Eq. (54) for various N atom Ge channels connected to Si contacts are shown in Fig. 5. The AMM transmission calculations are also shown in each panel of Fig. 5. The AMM transmission calculations only take into account transmission across the two Si–Ge interfaces on either end of the channel. The NEGF calculations, in addition to accounting for the interface transmission at the contact/channel interfaces, also take into account the partially reflected phonon waves from these interfaces that set up standing waves in the channel. These cause Fabry–Pérot-like oscillations in the channel, which are dependent on the length of the channel (the number of atoms N in the channel), as seen in the four examples shown in Fig. 5. Figure 5 shows transmission calculations for 3, 5, 10, and 50 atom channels. The number of oscillations in frequency space in the channel increases as N increases. Although evidence of these Fabry–Pérot oscillations in phonon transport has never been experimentally observed, it has been shown in other numerical studies.[24,37] This aspect of phonon interference follows naturally from phase coherent interference characteristic of the wave nature of phonon transport. This phase interference from the multiple reflection off the various interfaces is one of the major differences between this NEGF formulation and the semiclassical AMM approach, as discussed below.

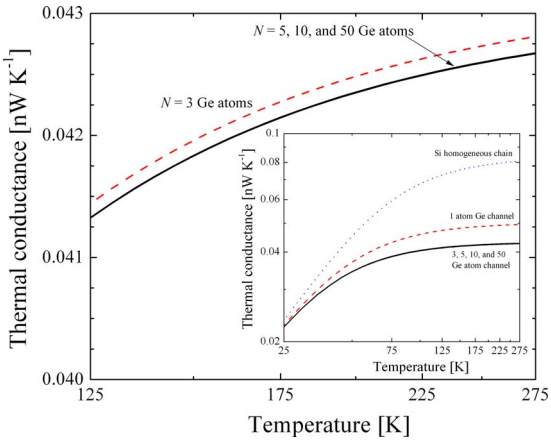

FIG. 6. (Color online) Thermal conductance calculations for N atom 1D chains using Eq. (47). The conductance of the 5, 10, and 50 atom Ge chains are identical and slightly less than the conductance of the three atom channel. The inset shows the N atom channels compared to the single atom channel and, for reference, the homogeneous Si chain. These results, which were derived from a "bottom-up" approach, are similar to those found by Zhang *et al.* (Ref. 24) which used a "top-down" derivation.

It is worth pointing out the physics that our simple implementation of AMM to double interfaces misses. Our approach was simply to multiply the individual interfacial transmissions to compute the combined transmission for AMM: $t^{\mathrm{AMM}}_{aba} = t^{\mathrm{AMM}}_{ab} t^{\mathrm{AMM}}_{ba}$. This expression misses two important pieces of physics: (a) it ignores *multiple reflections* between interfaces, which is needed to combine thermal impedances "bottom-up" and recover Fourier's law. Including multiple reflections would generalize this equation to yield $t^{\mathrm{AMM}}_{aba} = t^{\mathrm{AMM}}_{ab} t^{\mathrm{AMM}}_{ba} / (1 - r^{\mathrm{AMM}}_{ab} r^{\mathrm{AMM}}_{ba})$, where $r_{ab/ba}$ is the reflectivity. The modified equation, in effect, shows the conditions needed to scale the thermal conductance of large materials with length as one expects once the section length exceeds the scattering mean-free path; (b) even if we do include multiple reflections leading to the additivity of thermal impedances, it does not account for phase coherent interference of phonon waves that can actually make the impedance of a larger section smaller than the individual impedances. Such effects cannot be captured by the transmittivity, but with the complex transmission amplitude that accounts for the phase picked up during a pass of the phonon wave through the combined region. The transmittivity and reflectivity are the squares of the transmission and reflection amplitude.

Using the transmission calculations from Eq. (54) with Eq. (47) gives the thermal conductance for a multiple N atom channel, which is shown in Fig. 6, which compares the ther-

mal conductance of the various *N* atom Ge chains connected to Si contacts discussed in Fig. 5. The conductance of the 5, 10, and 50 atom Ge chains are identical and slightly less than the conductance of the three atom channel. The inset of Fig. 6 shows the *N* atom channels compared to the single atom channel and, for reference, the homogeneous Si chain. The conductance decreases from the one atom channel to the three atom channel (inset) and then further decreases from the three atom channel to the channels with more atoms (main part of graph), where it remains nearly constant. These are similar to results found by Zhang *et al.*,[24] only derived from a bottom-up approach, starting with a single atom.

In this work, since a 1D atomic chain is only considered, transverse modes are not taken into account and a very simple 1D spring potential is applied. Applying this to higher dimensional structures is as simple as specifying lattice points for given atoms in the different dimensions, applying the appropriate interatomic force in every direction, and then calculating the Green's functions for each atom in the system, realizing that now the Green's functions will take into account longitudinal and transverse interactions. Using this approach in higher dimensional systems enables thermal transport to be studied in the presence of planar or volumetric disorder or interatomic mixing in addition to multidirectional phonon scattering, which is a limitation of the semiclassical Boltzmann-based approaches. A future continuation of this basic walkthrough for NEGF formulation will include these higher dimensional calculations.

In addition to a low dimensional approach to NEGF, this work also considers completely harmonic phonon transport where scattering only occurs due to atomic junctions between atoms with two different masses and interatomic forces. Therefore, for an accurate comparison, the NEGF calculations are compared to a semiclassical AMM-based model derived for thermal boundary conductance between two atoms. This AMM-based model only accounts for scattering at interfaces and does not account for any other scattering in the atomic chains. However, the NEGF technique outlined in this paper can be extended to include various scattering events to model situations that semiclassically are modeled with more rigorous BTE-based models. For example, with the use of different, nonharmonic potentials and additional scattering times incorporated through additional scattering matrices,[27] various aspects of thermal transport can be modeled with NEGF such as three phonon processes (Normal or Umklapp), impurity scattering, or even electron-phonon scattering.

Although this work focused on comparing the NEGF technique to a semiclassical AMM-based model, this NEGF formalism offers a unique alternative to other, more computationally expensive phonon transport simulation tools, such as Monte Carlo or molecular dynamics simulations. The NEGF formalism can easily be extended to 3D crystal lattices and with appropriate definitions of crystal potentials, the quantum aspect of the wave nature of phonon transport can be studied with NEGF for various transport situations. However, the true power in this simulation tool will come with a combination of NEGF with other types of simulations methods. For example, using phonon scattering times determined from molecular dynamics simulations in NEGF calculations would prove an invaluable methodology to determine phonon conductance in novel nanostructures. This type of combinatory method of NEGF with other established tools will be a power tandem to truly understand quantum thermal transport phenomena.

V. CONCLUSIONS

With characteristic device sizes approaching atomic length scales, efficient tools for accurately predicting transport are becoming increasingly important for various applications. In this work, the semiclassical approach for modeling thermal transport is compared to the nonequilibrium Green's function formalism for a 1D atomic chain. The NEGF formalism is derived from a single atom in a bottom-up approach. The formalisms are identical when considering a homogeneous chain, but when introducing mass "impurities" in the chain, the two predict different results. Transmission across atomic junctions of mass impurities takes the form of the AMM in the semiclassical approach, which considers the transmission of a phonon flux across a single interface between two atoms. Using NEGF, however, the wave nature of phonon transport is captured in the transmission calculations and interference of phonon waves across an atom junction is observed by Fabry–Pérot-like peaks in the transmission predictions. The thermal conductance using NEGF for heat flow across atomic junctions is derived from a single atom and extended to a multiple atom chain, showing similar results to previous studies that modeled this problem with a top-down approach.

ACKNOWLEDGMENTS

Patrick Hopkins is grateful for funding from the LDRD program office through the Sandia National Laboratories Harry S Truman Fellowship. The authors would like to thank Rich Salaway, Jennifer Simmons, John Duda, and Justin Smoyer of the Microscale Heat Transfer Laboratory at U.Va. for insightful discussions. This work was supported in part by the Office of Naval Research through MURI Grant No. N00014-07-1-0723, and the NSF CAREER award, Grant No. 0748009. Sandia is a multiprogram laboratory operated by Sandia Corporation, a Lockheed–Martin Company, for the United States Department of Energy's National Nuclear Security Administration under Contract DE-AC04-94AL85000.

[1]D. G. Cahill, W. K. Ford, and K. E. Goodson, J. Appl. Phys. **93**, 793 (2003).
[2]W. A. Little, Can. J. Phys. **37**, 334 (1959).
[3]T. E. Beechem, S. Graham, P. E. Hopkins, and P. Norris, Appl. Phys. Lett. **90**, 054104 (2007).
[4]R. S. Prasher and P. E. Phelan, ASME Trans. J. Heat Transfer **123**, 105 (2001).
[5]P. E. Hopkins and P. M. Norris, J. Heat Transfer **131**, 022402 (2009).
[6]P. E. Hopkins and P. M. Norris, Nanoscale Microscale Thermophys. Eng. **11**, 247 (2007).
[7]G. Chen, Phys. Rev. B **57**, 14958 (1998).
[8]C. Dames and G. Chen, J. Appl. Phys. **95**, 682 (2004).
[9]P. E. Hopkins and P. M. Norris, ASME Trans. J. Heat Transfer **131**, 022402 (2009).
[10]S. Datta, *Electronic Transport in Mesoscopic Systems* (Cambridge Univer-

sity Press, Cambridge, 1995).
[11]H. Haug and A.-P. Jauho, *Quantum Kinetics in Transport and Optics of Semiconductors* (Springer, Berlin, 1996).
[12]R. van Leeuwen, N. E. Dahlen, G. Stefanucci, C.-O. Almbladh, and U. von Barth, Lecture Notes Phys. **706**, 33 (2006).
[13]K. Stokbro, J. Taylor, M. Brandbyge, and H. Guo, Lecture Notes Phys. **680**, 117 (2006).
[14]Y. Meir and N. S. Wingreen, Phys. Rev. Lett. **68**, 2512 (1992).
[15]A.-P. Jauho, N. S. Wingreen, and Y. Meir, Phys. Rev. B **50**, 5528 (1994).
[16]A. Dhar and D. Sen, Phys. Rev. B **73**, 085119 (2006).
[17]A. Bulusu and D. G. Walker, ASME Trans. J. Heat Transfer **129**, 492 (2007).
[18]K. Schwab, E. A. Henriksen, J. M. Worlock, and M. L. Roukes, Nature (London) **404**, 974 (2000).
[19]N. Mingo and L. Yang, Phys. Rev. B **68**, 245406 (2003).
[20]T. Yamamoto and K. Watanabe, Phys. Rev. Lett. **96**, 255503 (2006).
[21]J.-S. Wang, J. Wang, and N. Zeng, Phys. Rev. B **74**, 033408 (2006).
[22]A. Ozpineci and S. Ciraci, Phys. Rev. B **63**, 125415 (2001).
[23]W. Zhang, T. S. Fisher, and N. Mingo, ASME Trans. J. Heat Transfer **129**, 483 (2007).
[24]W. Zhang, T. S. Fisher, and N. Mingo, Numer. Heat Transfer, Part B **51**, 333 (2007).
[25]L. G. C. Rego and G. Kirczenow, Phys. Rev. Lett. **81**, 232 (1998).
[26]W. Zhang, N. Mingo, and T. S. Fisher, Phys. Rev. B **76**, 195429 (2007).
[27]S. Datta, *Quantum Transport: Atom to Transistor* (Cambridge Univeristy Press, Cambridge, 2006).
[28]G. Chen, ASME Trans. J. Heat Transfer **119**, 220 (1997).
[29]W. G. Vincenti and C. H. Kruger, *Introduction to Physical Gas Dynamics* (Krieger, Malabar, FL, 2002).
[30]A. Majumdar, ASME Trans. J. Heat Transfer **115**, 7 (1993).
[31]G. Chen, *Nanoscale Energy Transport and Conversion: A Parallel Treatment of Electrons, Molecules, Phonons, and Photons* (Oxford University Press, New York, 2005).
[32]Y. Imry and R. Landauer, Rev. Mod. Phys. **71**, S306 (1999).
[33]G. Chen, Appl. Phys. Lett. **82**, 991 (2003).
[34]C. Kittel, *Introduction to Solid State Physics*, 7th ed. (Wiley, New York, 1996).
[35]W. A. Harrison, *Electronic Structure and the Properties of Solids: The Physics of the Chemical Bond* (Freeman, San Francisco, 1980).
[36]D. E. Gray, in *American Institute of Physics Handbook*, 3rd ed. (McGraw-Hill, New York, 1972).
[37]P. Hyldgaard, Phys. Rev. B **69**, 193305 (2004).